Silicon (2022) 14:481–492
https://doi.org/10.1007/s12633-020-00842-2

ORIGINAL PAPER

Impact Resistance and Strength Development of Fly Ash Based Self-compacting Concrete

Selvaraj Kumar[1] · Palanisamy Murthi[2] · Paul Awoyera[3] · Ravindran Gobinath[2] · Sathis kumar[4]

Received: 24 September 2020 / Accepted: 12 November 2020 / Published online: 19 November 2020

Abstract

The development of self-compacting concrete using alternative materials is expanding in recent years due to the technical and economic benefits of the mixture. This study focuses on the structural and compositional behavior of sodium hydroxide (NaOH)-activated fly ash based self-compacting concrete (SCC). Fly ash was partially replaced with Ordinary Portland Cement from 0–30%. The tests performed on concrete samples include workability, strength, microstructural, and impact resistance. The results showed that activated fly ash reduces the heat of the hydration process of the concrete mixture but enhances pozzolanic reactions, which led to increased strength properties. The addition of activated fly ash modifies the mineralogy of the concrete, as evident in strength characteristics. The best performance of the activated fly ash based SCC, in terms of strength, was found at 10–15% substitutions, which can somewhat reduce the cost of production of SCC and strength improvement advantage.

Keywords Activated fly ash · pozzolan · Self-compacting concrete · Sodium hydroxide · Structural behavior

1 Introduction

Among several factors, the overall performance of a concrete structure, during construction or in service, largely depends on the material composition. The raw concrete materials influence its workability, strength development, morphology, and mineralogical composition [1]. In recent years, there have been advancements in concrete technology, as numerous alternative materials are investigated continuously for possible use in concrete production. The alternative materials are mostly introduced as binders or aggregate in the cementitious matrix.

Fly ash, a byproduct of coal-burning process, has application in raw or activated form as a concrete constituent [2]. Fly ash has been utilized as a partial replacement of Portland cement or as a cement admixture in concrete. With the use of fly ash, studies [3–7] have reported that pore structure, hydration, phase change, mineralogy, and strength properties of concrete were enhanced. The performance of fly ash in concrete depends principally on its fineness, carbon content, and reactivity [8, 9]. Other researches that focused on fly ash concrete have reported that: fly ash is suitable for reducing water absorption characteristics and corrosion risk in recycled aggregate concrete [10]; addition of fly ash to concrete promotes early strength development of the matrix [11]; and that fly ash improves thermal insulator properties of wall plasters [12].

Self-compacting concrete (SCC), owing to its highly flowable nature under self-weight (without segregation), has been widely accepted for construction in difficult sites, such as having sloppy terrain or with congested reinforcements. The application of SCC cuts across sections with congested reinforcement bars or in sloped sites. Several applications of SCC produced using fly ash have been reported [13–16]. With fly ash incorporation in SCC as a partial replacement in range of 30–65% by weight of cement, sorptivity in concrete was reduced [17], and high volume fly ash also significantly decreased both drying and autogenous shrinkage in concrete [18]. Based on the findings of previous studies, fly ash self-compacting concrete performs comparably well with the conventional concrete mix (without fly ash) in terms of strength [19, 20]. However, fly ash SCC has a better attribute in heat resistance, sorptivity, and shrinkage reduction than the conventional mixes [21].

✉ Paul Awoyera
paul.awoyera@covenantuniversity.edu.ng

[1] Research Scholar, Anna University, Chennai, India

[2] S R Engineering College, Warangal, Telangana, India

[3] Department of Civil Engineering, Covenant University, Ota, Nigeria

[4] Jay Shriram Group of Institutions, Tirupur, Tamil Nadu, India

Table 1 Physical properties of aggregates

Properties	Cement	Fly ash	M-sand	Crushed rock
Fineness modulus	3.30	7.20	2.08	
Specific gravity	3.15	2.9	2.5	2.77
Water absorption			1.32	0.42
Impact value				25
Abrasion				28
Crushing value				7.60
Specific surface area (cm^2/gm)	2325	2453.3		

Despite the number of researches focusing on the use of fly ash in concrete or with fly based self-compacting concrete, yet there are still significant contributions to be made in this area. There are variances in the method of activation of fly ash in concrete. Also, the impact of microstructural modifications on the strength properties has not been overly explored. Therefore, the present study dwelt on NaOH–activated fly ash as a partial replacement of Portland cement for the production of SCC. Using fly ash in SCC has better value. The presence of calcium hydroxide in Portland cement concrete makes it susceptible to acid attack, resulting in corrosion of embedded steel. In other studies [11, 22–26], fly ash activation was achieved by using sodium hydroxide (NaOH), lime ($Ca(OH)_2$), Na_2SO_4, and sodium silicate (Na_2SiO_3). The process involves geo polymerization of the fly ash, which will act as a binder. However, fly ash is not only used as a binder in this study but also as additional pozzolanic material with increased surface area, thus targeting enhancement of certain characteristics of concrete such as improved permeability reduction, increased toughness and increased impact resistance.

2 Materials and Method

2.1 Materials

The materials utilized for the study were: grade 53 Portland pozzolanic cement, manufactured sand, crushed rock, polycarboxylate ethers chemical admixture-suitable for self-compacting concrete, and fly ash. Table 1 shows the physical properties of the aggregates.

Manufacture sand (M-sand), obtained from crushing of hard granite, was used as fine aggregate. Previous experimental works have shown that M-sand improves the binding property of concrete paste [27, 28]. M-Sand that passed through 4.75 mm aperture and retained on 60 microns sieve was used, as per IS2386 [29] criteria. Crushed rock particles with size range 10 to 12 mm, was used as coarse aggregate. Potable water with pH value 7.0 was used for concrete mixing. Class F fly ash, obtained by burning anthracite or bituminous coal, was utilized as a partial replacement of cement. Table 2 presents the oxide composition of fly ash and cement used in this study, as obtained from parallel studies [30, 31]. As shown, the lime (CaO) content of the fly ash is less than 7%, and at this level, the fly ash will provide more pozzolanic influence in the concrete [32].

2.2 Method

In this study, an M30 grade of concrete was designed and tested following established procedures. Table 3 shows the mix proportion for the constituent materials.

Fly ash was activated using NaOH solution. A 10 Molarity NaOH of 400gms was mixed thoroughly with one litre of demineralized water in a non-reactive plastic drum, and 50 litres of the resulting solution was found suitable to activate 250 kg of fly ash.

The fly ash was immersed in NaOH for 24hrs, and it gradually hardens up in the process (increasing the specific surface area and also alters the chemical characteristics of fly ash). The whole reaction is exothermic in nature, which was due to to the dissolution of NaOH pellets, thus liberating a lot of heat in the process. The hardened fly ash was pulverized with

Table 2 Oxide composition of the fly ash used

Oxides	SiO_2	Al_2O_3	Fe_2O_3	CaO	MgO	Na_2O	K_2O	P_2O_5	TiO_2	LOI
Fly ash (wt%)	50.0	28.25	13.5	1.79	0.89	0.32	0.46	0.98	1.54	0.64
Cement (wt%)	24.09	19.47	6.27	74.21	3.19	1.74	0.84	1.13	0.61	

Table 3 Mix proportions

Mix	Cement (kg/m^3)	Fly ash (kg/m^3)	M-sand (kg/m^3)	Granite (kg/m^3)	Water (kg/m^3)	Super plasticizers (kg/m^3)
SCCF0	470	0	962.8	727.84	183.3	3.76
SCCF10	423	47	962.8	727.84	183.3	3.76
SCCF15	399.5	70.5	962.8	727.84	183.3	3.76
SCCF20	376	94	962.8	727.84	183.3	3.76
SCCF25	352.5	117.5	962.8	727.84	183.3	3.76
SCCF30	329	141	962.8	727.84	183.3	3.76

a ball mill and sieved through a 90-micron sieve. The resulting sieved fly ash was stored in a closed container prior to its use.

Scanning Electron Microscope (SEM) was used to observe the morphology of fly ash, activated fly ash, and selected concrete mix (based on higher strength value). Also, Fourier-transform infrared spectroscopy, a technique that is used to obtain an infrared spectrum of absorption or emission of a solid, liquid, or gas, was used to assess fly ash, activated fly ash, and selected concrete mix. An FTIR spectrometer simultaneously collects high- spectral resolution data over a wide range.

Preparation and testing of the self-compacting concrete described in this study follow the EFNARC specification and guidelines for SCC [33]. The workability/rheology tests performed, with the standard limits, are listed in Table 4. The concrete samples prepared include cubes of 150 mm dimensions (for compressive strength tests), cylinders of 150 length x 300 mm diameter (split tensile strength tests), beams of 150 × 200 × 1200 mm (for flexural strength tests). The samples were cured by immersion in water for 28 days. In all, 36 concrete cubes, 18 concrete cylinders, and 18 reinforced concrete beams were produced. Cubes were tested in triplicates, and cylinders in duplicates, at 7 and 28 days. At the same time, beams were tested in duplicates at 28 days. The averages of the strength of samples were taken as the corresponding concrete mix strength.

The compressive strength and split tensile strength of the 150 mm cube and 150 × 300 mm cylinders, respectively, were determined using a compression testing machine of 2000 KN capacity in line with IS 516 [34] criteria. Direct measurement of the tensile strength of concrete is somewhat cumbersome in that there are no testing apparatus that has been designed, which assure uniform distribution of the pull applied to the concrete. This is also sometimes referred as, Brazilian Test. However, the test was performed by placing a cylindrical specimen horizontally between the loading surfaces of a compression testing machine, and the load is applied until failure of the cylinder, along with vertical diameter occurs.

The flexural strength of 150 mm x 200 mm x 1200 mm beams was determined using the Universal testing machine (UTM), with a four-point arrangement. Figures 1 and 2 show the reinforcement details and flexural test on a typical beam, respectively.

All dimensions are in cm.

Wire mess (area of 3 cm^2) reinforced slab panels (600 × 600 × 50 mm) were prepared from all mixtures. Upon completion of curing (28 days immersion in water), slabs were subjected to drop weight tests following the guidelines described by Sateshkumar et al. [31]. The test requires a repeated application of impact load in the form of blows, using an 83.385 N hammer falling from 850 mm height on the center of the slab. The number of blows resulting in the initiation of first crack and blows required for the final failure of slab was noted. A slab subjected to impact test is shown in Fig. 3.

2.3 Poisson's Ratio

A compressometer, with 5 mm dial gauge travel by 0.001, was utilized to determine the stress/strain ratio (modulus of elasticity) of concrete cylinders of 10–15 cm diameter during compression testing. An extensometer was used to determine both axial and radial strain in cylindrical concrete specimens during the compression test, through which the Poisson's ratio

Table 4 Workability (rheology) properties of SCC

Method	Property	Requirement as per [33]	Class
Slump flow (mm)	Filling ability	550–650	SF1
		660–750	SF2
		760–850	SF3
V-Funnel (s)	Filling ability	≤ 8	VF1
		9–25	VF2
L-box (mm)	Passing ability	≥ 0.8 with 2 rebars	PA1
		≥ 0.8 with 3 rebars	PA2

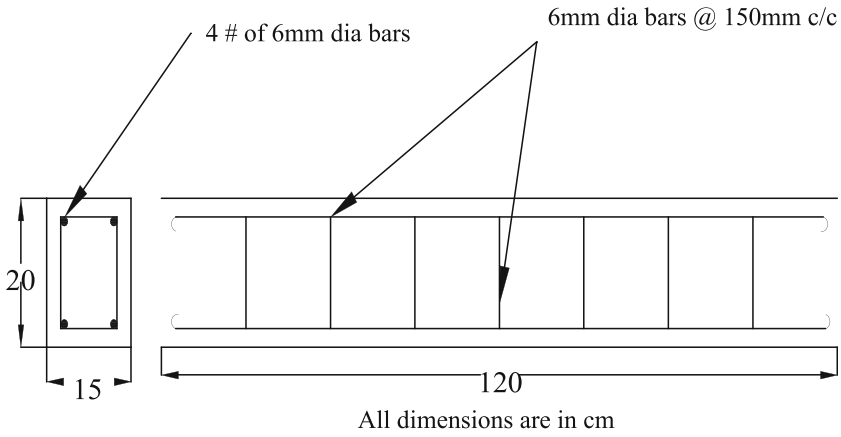

Fig. 1 Beam reinforcement details

was obtained. This study followed the ASTM C 469 [35] procedures, which describes the use of compressometer on a cylindrical specimen for the test. This device is equipped with a sensor that measures and amplifies vertical deformation.

3 Results and Discussion

3.1 Workability Tests

Figure 4 shows the results of workability tests performed on fresh concrete mixtures. In the slump flow test (Fig. 4a), all the mixtures were within the EFNARC SF2 limit. Consequently, the concrete samples can be regarded as sound in terms of their ability to fill up form works. According to EFNARC [33], concrete in this category is fit for normal applications. Figure 4b shows the V-funnel data. As shown, both control concrete (SCCF0) and mix with 10% fly ash (SCCF10) were within the VF2 category, thus implying that there was increasing flow time in the mixture, and it is more likely to exhibit thixotropic effects [33], a helpful condition for limiting the formwork pressure or improving segregation resistance. Other mixtures were within the VF1 category (Table 4), which is an indication that the concrete had good filling ability, which may be beneficial in areas having congested reinforcement [33]. However, bleeding and segregation may be the only set back for these mixes. This performance may be attributed to increased water absorption as fly ash content is increased. These mixtures can be improved through the addition of a considerable amount of superplasticizer.

The L-box data is shown in Fig. 4c. This test assesses the flow of concrete, and also the extent to which the concrete is subjected to blocking by reinforcement. As can be seen, the L-box values or blocking ratio of the mixes (SCCF15, SCCF20, SCCF25 and SCCF30) were found to be within the PA1/PA2 limit (Table 4), whereas both the control and SCCF10 were below this limit. Based on this data, it is confirmed that the increased content of activated fly ash enhanced the blocking ratio of the mixes. These results agree with that of a related study [36], where a positive influence of fly ash on the workability of SCC has been reported.

Fig. 2 Flexural test (Beam)

Fig. 3 Slab under impact load test

3.2 Strength and Poisson Ratio Evaluation of Tested Hardened SCC

Testing hardened concrete plays a vital role in controlling and confirming the quality of cement concrete works. The compressive strength test is needed in cases where strength in tension or in shear is of primary importance. Figure 5 presents the strength properties of the concrete samples. The compressive strength of cubes (Fig. 5a) increased with respect to the addition of activated fly ash up to 15%, the strength that surpassed that of the concrete mix at both 7 and 28 days. However, a further increase in activated fly ash content reduced the strength gradually. There was a reduction in compressive strength beyond 15% fly ash substitution, and this was also the case reported in another study [37]. The drop in strength may be because silica mineral was increased in the concrete matrix; thus, reducing the hydration rate, yet without enough curing period to allow complete pozzolanic actions. A prolonged curing process for this concrete could improve its strength performance.

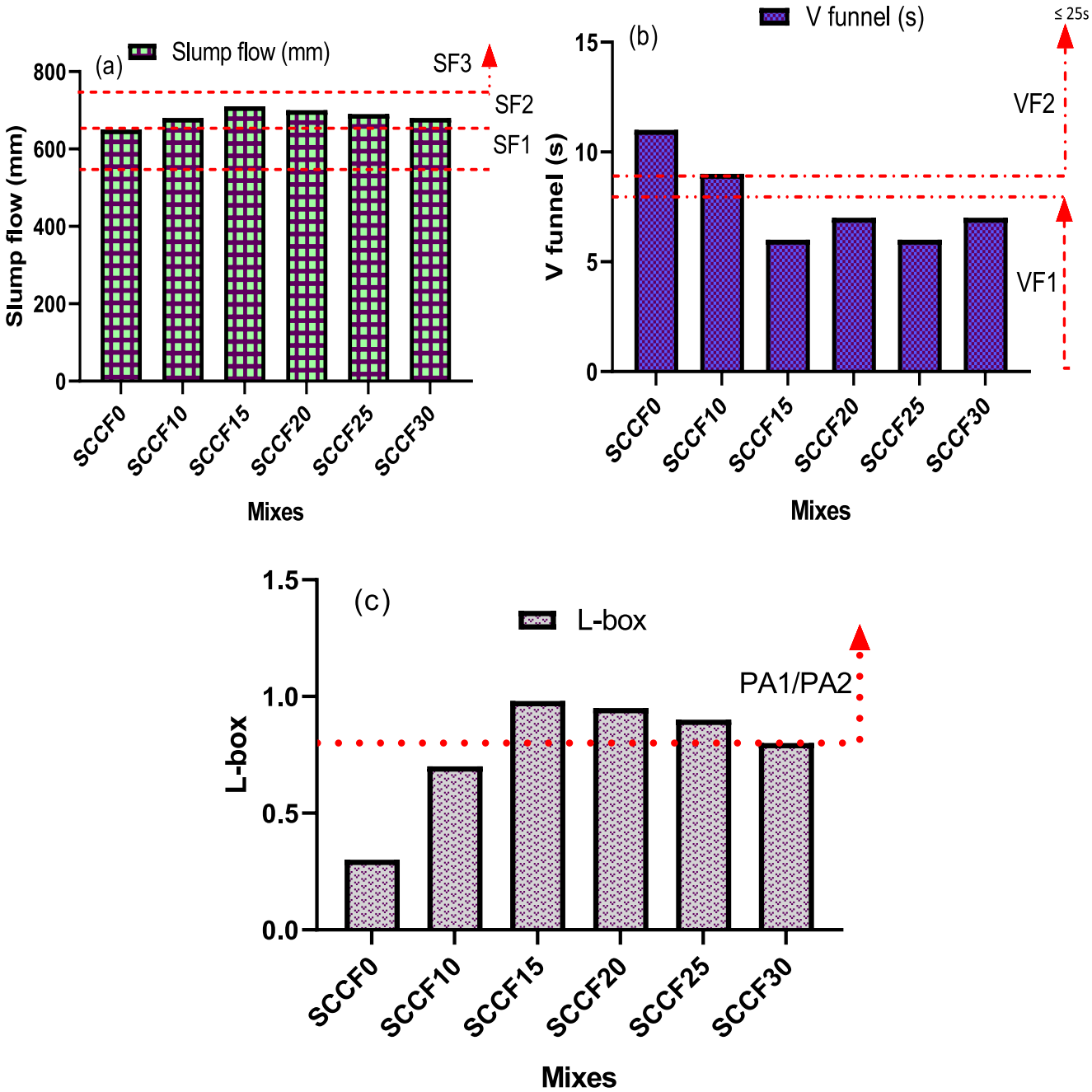

Fig. 4 Workability test data (**a**) slump flow (**b**) V funnel (**c**) L-box

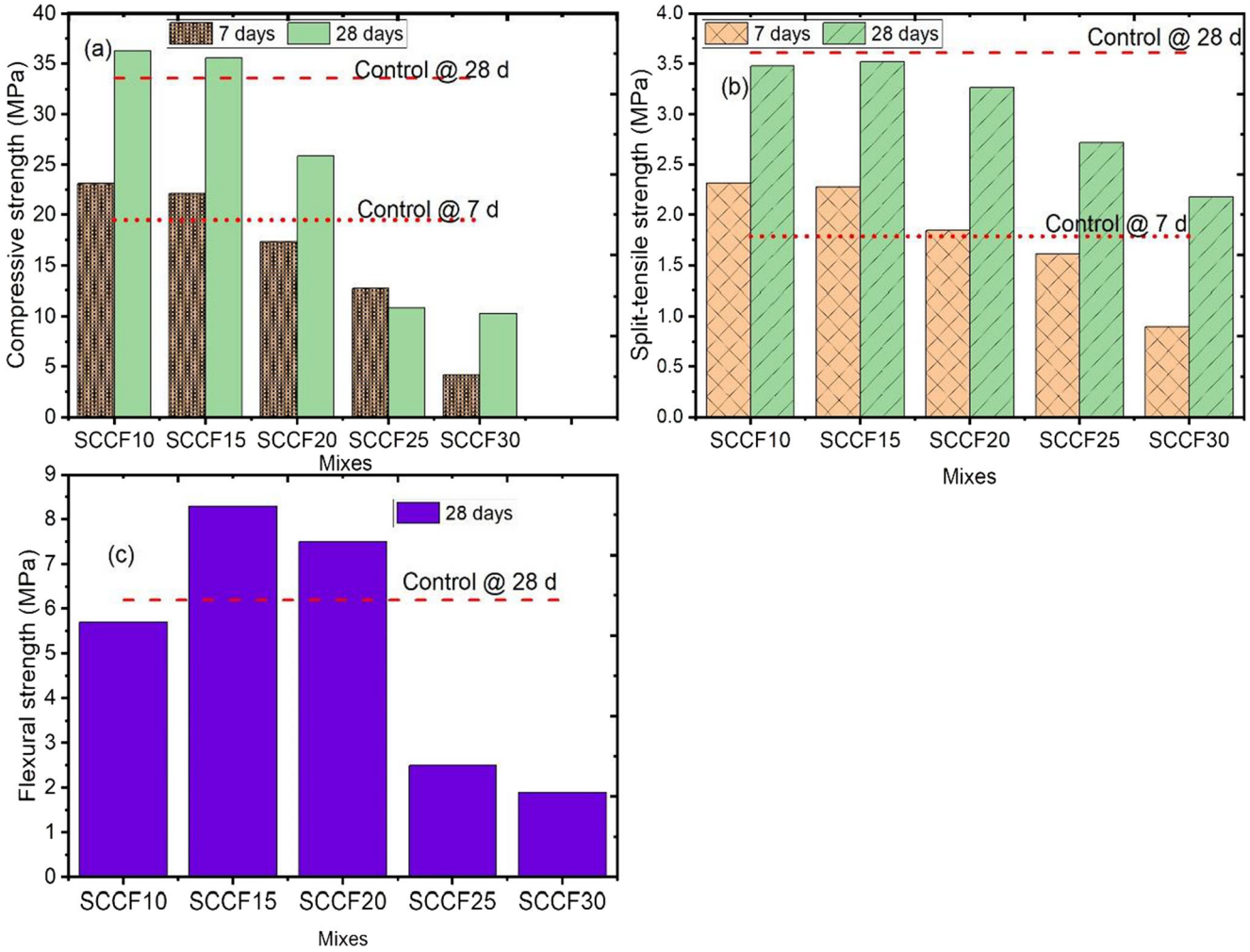

Fig. 5 Strength properties of concrete (**a**) compressive strength (**b**) split- tensile strength (**c**) flexural strength

For the split-tensile strength (Fig. 5b), the result shows that 10% and 15% activated fly ash replaced concrete produced maximum split tensile strength over

Table 5 Load – deflection data

Mix	Left		Centre		Right	
	load (ton)	Deflection	load (ton)	deflection (mm)	Load (ton)	Deflection (mm)
SCCF0	3.20	1.15	3.00	1.20	3.20	1.30
SCCF10	3.00	2.80	3.00	2.40	3.00	2.60
SCCF15	4.90	0.90	4.50	0.90	4.90	0.80
SCCF20	5.00	2.50	5.00	1.50	5.00	1.70
SCCF25	3.60	3.00	3.60	3.00	3.00	3.10
SCCF30	3.40	1.50	3.40	1.50	3.40	0.50

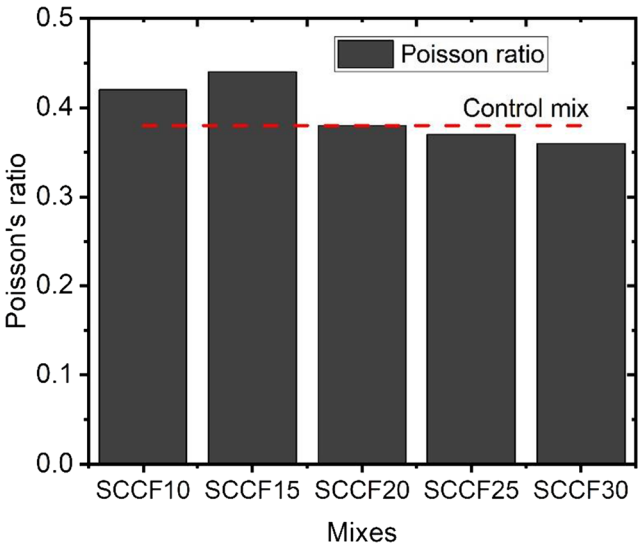

Fig. 6 Poisson's ratio

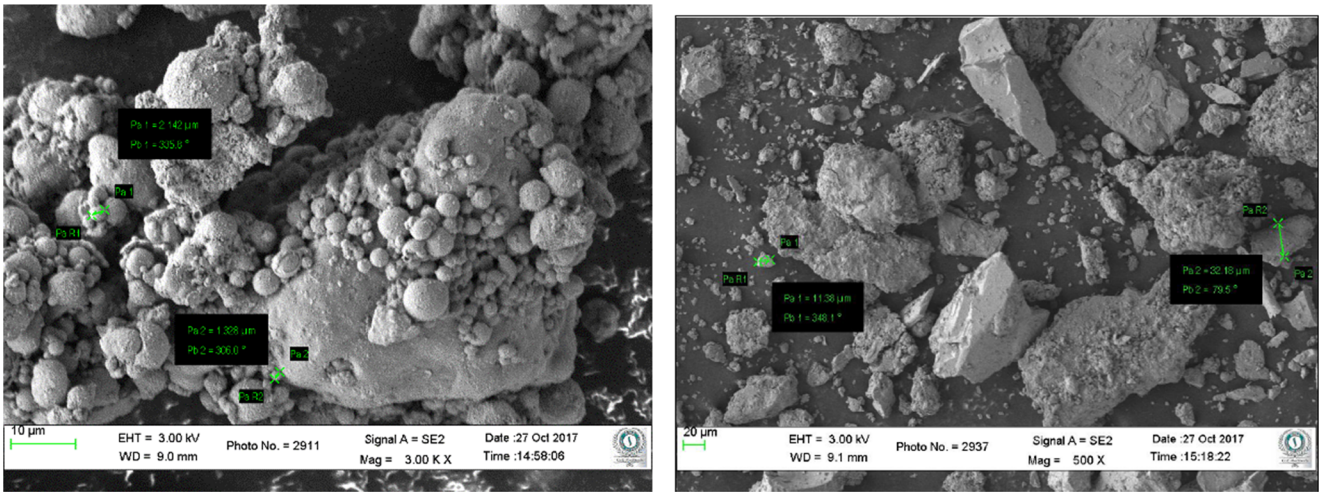

Fig. 7 SEM morphology (**a**) fly ash (**b**) activated fly ash

the conventional concrete. Similar behavior was noted in the compressive strength values.

Flexural strength is presented in Fig. 5c. Higher values were obtained at 15%, and 20% activated fly ash substitution for cement in the concrete than the control mix.

The load-deflection at specific points in the beams are noted in Table 5. As evident in the strength results, better load resistance was provided by mixtures containing 15% fly ash (SCCF15) and 20% fly ash (SCCF20). These results suggest that, at that fly ash substitution level, the ductility of the beams was increased.

Poisson's ratio, a ratio of lateral strain to longitudinal strain, was calculated for all the concrete mixtures. Figure 6 shows the Poisson ratio for the concrete mix tested. The value of Poisson's ratio varied from 0 to 0.5. The Poisson ratio takes a similar trend as the cube and cylinder strengths, in that, only at 10% and 15% fly ash substitution that the concrete responds to stress than in the control concrete.

3.3 Morphology and Mineralogy of Concrete

Figure 7 shows the SEM morphologies of fly ash and activated fly ash. The SEM images revealed that the fly ash particles are spherical in shape (Fig. 7a), while the activated fly ash particles are elongated and angular in shape (Fig. 7b) (a result of persistent burning).

The SEM images of the concrete is presented in Fig. 8. structure and pores of the concrete are varied, and it was found that the size of the pores of the concrete is larger in normal concrete (Fig. 8a), than in Alkali activated flyash concrete mix of 20%

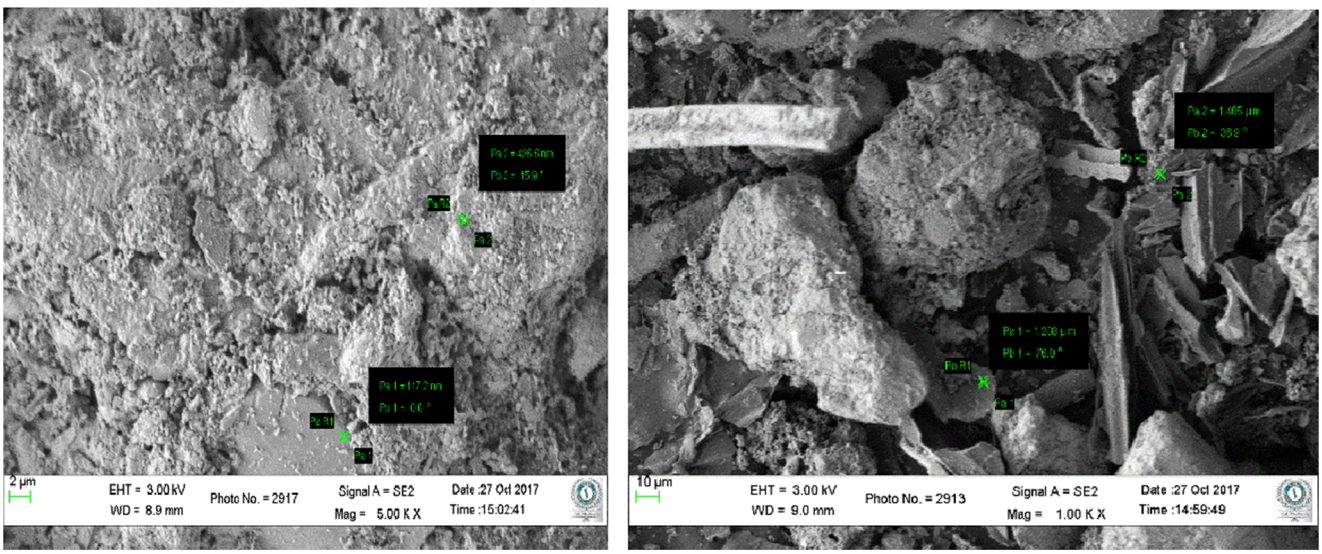

Fig. 8 SEM morphology of concrete (**a**) control (**b**) 20% activated fly ash concrete

replacement (Fig. 8b). The roundness and smaller size of the particles was calculated as 2.047, which represents that the particles are angular in shape. Because higher values of roundness implies that material is angularly shaped [38]. Thus, better packing is created between the particles and reduces porosity in the matrix. Therefore, the strength of the mix was enhanced.

The FTIR analysis helps to find the bond formation in the concrete and also to find the chemical

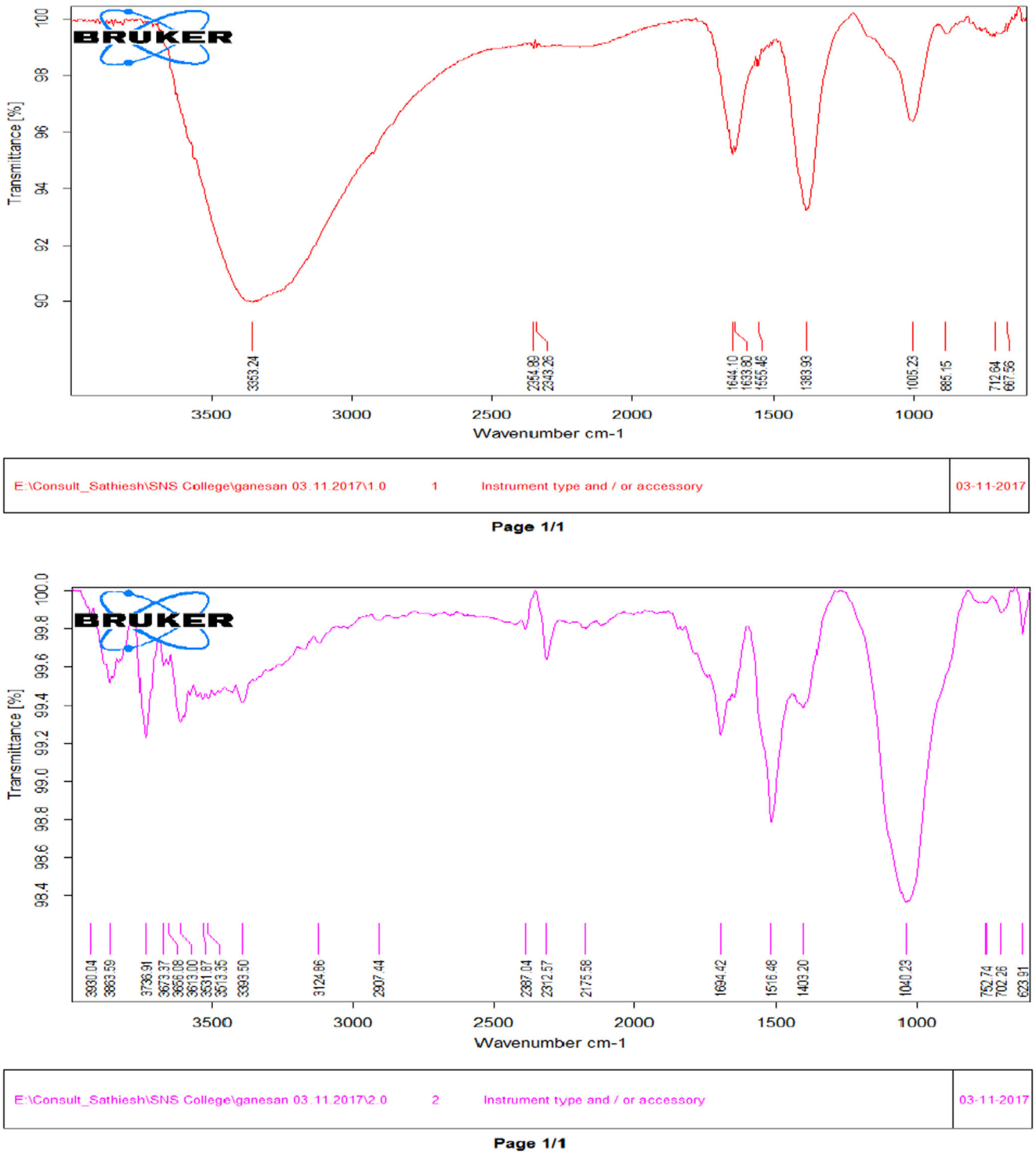

Fig. 9 FTIR of Fly ash (**a**) Fly ash (**b**) activated fly ash

composition indirectly. Figure 9 shows the FTIR of fly ash (Fig. 9a) and activated fly ash (Fig. 9b).

The data reveals the highest transmittance of 3353 cm^{-1}, which indicates stretching of the OH bond, and the presence of phenol, then 1383 cm^{-1} represents the presence of C - H bonding in the methylene group. The two components appearing at around 1090 cm^{-1} and 1140 cm^{-1} could be equated to the band's characteristic of the silicon tetrahedral in a silica-rich gel. That is, there was a deconvolution of this main band in the sample.

In Fig. 9b, the data indicate that activation of fly ash increased the formation of Si-O-Si Bond, which is observed from the transmittance value of 1043 cm-^{1}. The peak

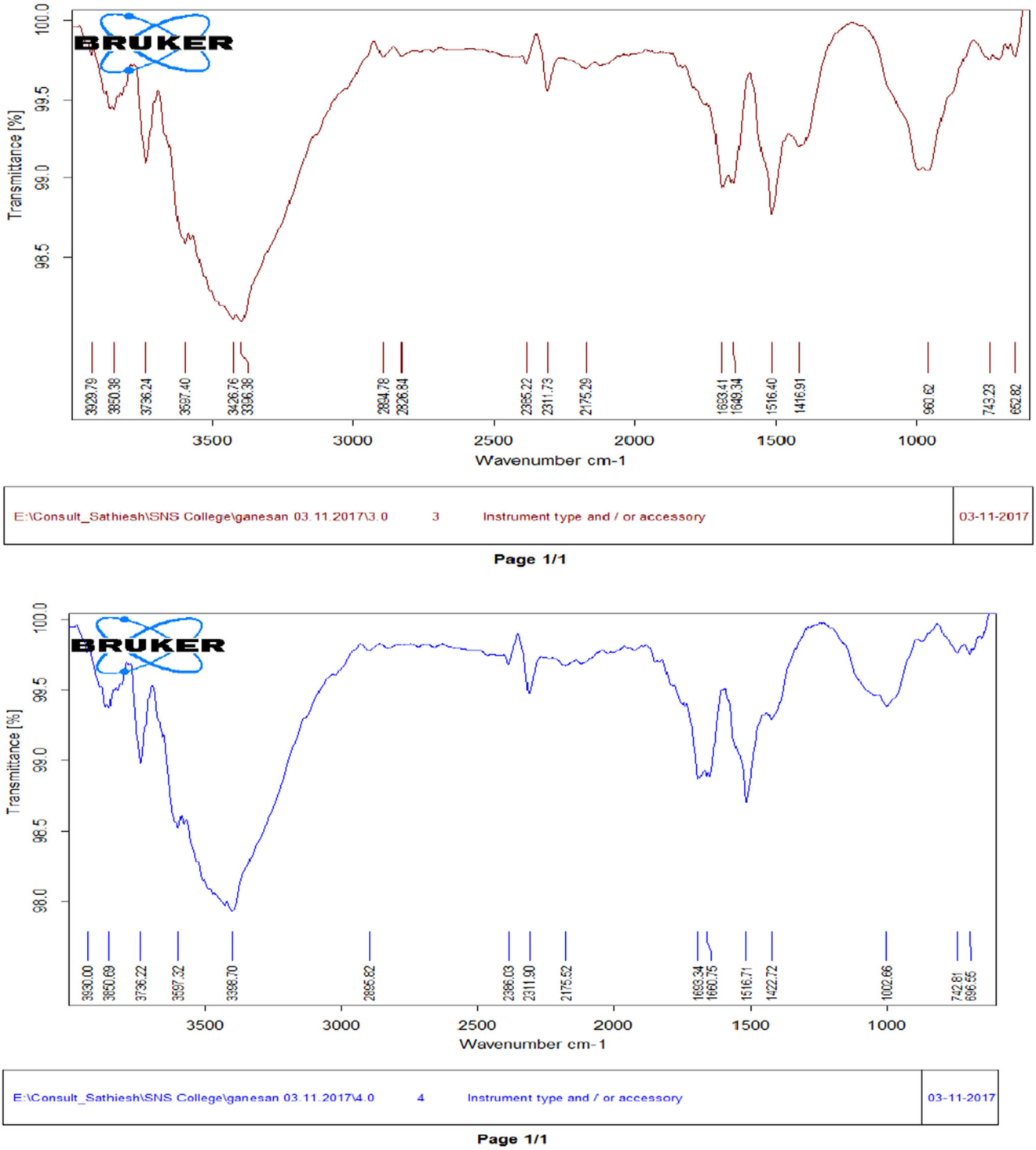

Fig. 10 FTIR spectra (**a**) Control concrete (**b**) 20% activated fly ash concrete

corresponding to portlandite (narrowband at around 3635 cm-1 typical of O–H stretching vibrations), for instance, disappeared after the NaOH was added.

Figure 10 shows the FTIR data of control concrete (Fig. 10a), and 20% fy ash substitution mix (Fig. 10b). There was no change in the bond formation, but only the C-S-H gel formation was observed due to the transmittance value of 3390 cm^{-1}. The value 1422 cm^{-1} has been observed where C-H bond formation is dominant. The FTIR spectrum for SCCF20 pastes contained a narrow band at 3640 cm-1, associated with the O–H stretching.

Vibrations in Portlandite. Another band was detected at around 974 cm-1, which is attributable to the stretching vibrations in the Si–O bonds (Si–O) in the SiO_4 tetrahedral that comprise the C-S-H gel, and a third at 760 cm^{-1}, assigned to (O–Si–O) bending.

Vibrations. The band at around 967–971 cm^{-1} on the FTIR spectra represent NaOH. Hence, OH groups in the range of 3350 cm^{-1} indicate the resultant product of hydration as $Ca(OH)_2$ and a then small amount of a silica gel precipitated with the C–S–H gel during synthesis was observed.

3.4 Impact Resistance

The impact resistance of the concrete mixes is presented in Fig. 11. The performance of the concrete was measured in terms of the number of blows at first crack appearance and failure. As shown on the plot, the activated fly ash concrete, at 10% and 15% fly ash substitution levels, have better impact resistance than other mixes. Higher impact resistance developed in SCCF10 and SCCF15 could be associated with reduced permeability of concrete, resulting from the pozzolanic effect of activated fly ash at this level. Thus, activated fly ash can be used as a convincing substitution for cement.

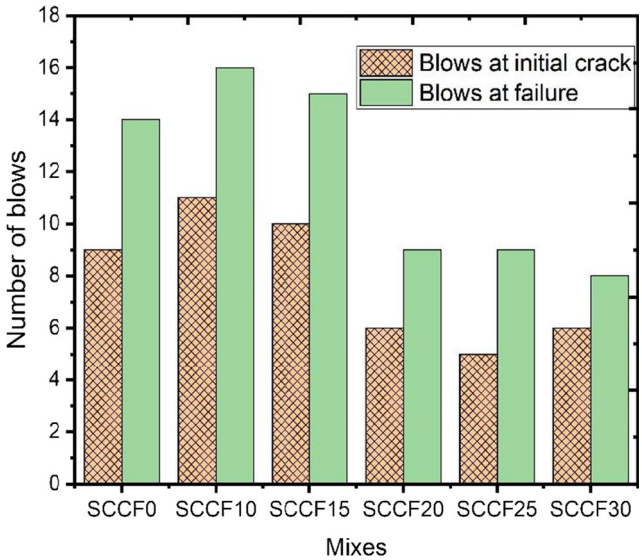

Fig. 11 Impact resistance of concrete mixes

4 Conclusion

This study focuses on the structural and compositional behavior of NaOH-activated fly ash concrete. The tests performed on concrete samples include workability, strength, microstructural, and impact resistance. The following conclusions were drawn from the study:

a. Activated fly ash reduced the heat of the hydration process, but exhibited pozzolanic charateristics, thereby increasing the strength of the concrete. The investigation shows that the additions of activated fly ash in concrete increase both physical and mechanical properties.
b. In fresh concrete assessment, workability increased with an increase in activated fly ash content. The workability and filling ability of self- compacting concrete tested are considerably increased with the addition of superplasticizer, overall falls within the acceptable limits.
c. Based on mechanical properties, mixes SCCF10 and SCCF15, having 10% and 15% activated fly ash, respectively, as a cement replacement, gave maximum strength value under different testing methods.
d. There is a gradual increase in impact strength up to 15%, but further replacements cause a reduction in strength of the concrete. The reason for this high material strength is due to the formation of C-S-H gel activation in alkali-activated fly ash concrete.
e. The SEM morphology revealed wide surface particles in the alkali activated fly ash concrete, which reflects in the certain higher mechanical strength obtained. Also, the FTIR analysis revealed the formation of C-S-H, observed with a small amount of Si-O-Si gel for both control and Alkali Activated fly ash concrete.

Acknowledgements The authors hereby acknowledge the support received from the KPR Institute of Engineering and Technology, Tamilnadu, India, during the execution of this project.

Author Contributions All authors whose names appear on the submission made substantial contributions to the conception, design of the work, acquisition, analysis, interpretation of data and wrting/revision of the article.

Data Availability Data used in this study will be made available upon request.

Compliance with Ethical Standards

Conflict of Interest The authors declare that there is no conflict of interest.

Consent to Participate Not applicable.

Consent for Publication Not applicable.

References

1. Murthi P, Awoyera P, Selvaraj P et al (2018) Using silica mineral waste as aggregate in a green high strength concrete: workability, strength, failure mode, and morphology assessment. Aust J Civ Eng 0:1–7. https://doi.org/10.1080/14488353.2018.1472539
2. Guo Y, Zhang Y, Soe K et al Effect of fly ash on mechanical properties of magnesium oxychloride cement under water attack. Struct Concr n/a. https://doi.org/10.1002/suco.201900329
3. Chindaprasirt P, Jaturapitakkul C, Sinsiri T (2005) Effect of fly ash fineness on compressive strength and pore size of blended cement paste. Cem Concr Compos 27:425–428. https://doi.org/10.1016/j.cemconcomp.2004.07.003
4. Liu J, Qiu Q, Xing F, Pan D (2014) Permeation properties and pore structure of surface layer of fly ash concrete. Materials (Basel) 7: 4282–4296. https://doi.org/10.3390/ma7064282
5. Feng J, Liu S, Wang Z (2015) Effects of ultrafine fly ash on the properties of high-strength concrete. J Therm Anal Calorim 121: 1213–1223. https://doi.org/10.1007/s10973-015-4567-3
6. Islam MM, Alam MT, Islam MS (2018) Effect of fly ash on freeze–thaw durability of concrete in marine environment. Aust J Struct Eng 19:146–161. https://doi.org/10.1080/13287982.2018.1453332
7. Benli A Mechanical and durability properties of self-compacting mortars containing binary and ternary mixes of fly ash and silica fume. Struct Concr. https://doi.org/10.1002/suco.201800302
8. Chousidis N, Ioannou I, Rakanta E et al (2016) Effect of fly ash chemical composition on the reinforcement corrosion, thermal diffusion and strength of blended cement concretes. Constr Build Mater 126:86–97. https://doi.org/10.1016/j.conbuildmat.2016.09.024
9. Meesala CR, Verma NK, Kumar S Critical review on fly-ash based geopolymer concrete. Struct Concr. https://doi.org/10.1002/suco.201900326
10. Kurda R, de Brito J, Silvestre JD (2019) Water absorption and electrical resistivity of concrete with recycled concrete aggregates and fly ash. Cem Concr Compos 95:169–182. https://doi.org/10.1016/j.cemconcomp.2018.10.004
11. Hefni Y, Zaher YA, El, Wahab MA (2018) Influence of activation of fly ash on the mechanical properties of concrete. Constr Build Mater 172:728–734. https://doi.org/10.1016/j.conbuildmat.2018.04.021
12. Bicer A (2018) Effect of fly ash particle size on thermal and mechanical properties of fly ash-cement composites. Therm Sci Eng Prog 8:78–82. https://doi.org/10.1016/j.tsep.2018.07.014
13. Singh N, Singh SP (2016) Carbonation resistance and microstructural analysis of low and high volume fly ash self compacting concrete containing recycled concrete aggregates. Constr Build Mater 127:828–842. https://doi.org/10.1016/j.conbuildmat.2016.10.067
14. Ushaa T, Anuradha R, Venkatasubramani G (2015) Performance of self-compacting geopolymer concrete containing different mineral edmixtures. Indian J Eng Mater Sci 22:473–481
15. Senthamilselvi R, Revathi P (2019) Influence of blended cement on the fresh properties of self-compacting concrete incorporating recycled aggregate. In: Rao ARM, Ramanjaneyulu K (eds) Recent advances in structural engineering. Springer Singapore, Singapore, pp 907–919
16. Mohammed MK, Dawson AR, Thom NH (2013) Production, microstructure and hydration of sustainable self-compacting concrete with different types of filler. Constr Build Mater 49:84–92. https://doi.org/10.1016/j.conbuildmat.2013.07.107
17. Leung HY, Kim J, Nadeem A et al (2016) Sorptivity of self-compacting concrete containing fly ash and silica fume. Constr Build Mater 113:369–375. https://doi.org/10.1016/j.conbuildmat.2016.03.071
18. Kristiawan SA, Aditya MTM (2015) Effect of high volume fly ash on shrinkage of self-compacting concrete. Procedia Eng 125:705–712. https://doi.org/10.1016/j.proeng.2015.11.110
19. Mahalingam B, Nagamani K, Kannan LS et al (2016) Assessment of hardened characteristics of raw fly ash blended self-compacting concrete. Perspect Sci 8:709–711. https://doi.org/10.1016/j.pisc.2016.06.066
20. Adesina A, Awoyera P (2019) Overview of trends in the application of waste materials in self-compacting concrete production. SN Appl Sci 1:962. https://doi.org/10.1007/s42452-019-1012-4
21. Çelik Z, Bingöl AF Mechanical properties and postcracking behavior of self-compacting fiber reinforced concrete. Struct Concr. https://doi.org/10.1002/suco.201900396
22. Palacios M, Alonso MM, Varga C, Puertas F (2019) Influence of the alkaline solution and temperature on the rheology and reactivity of alkali-activated fly ash pastes. Cem Concr Compos 95:277–284. https://doi.org/10.1016/j.cemconcomp.2018.08.010
23. Stolz J, Boluk Y, Bindiganavile V (2018) Mechanical, thermal and acoustic properties of cellular alkali activated fly ash concrete. Cem Concr Compos 94:24–32. https://doi.org/10.1016/j.cemconcomp.2018.08.004
24. Singh GI, Deshwal B, Bhattacharyya S (2018) Effect of sodium carbonate/sodium silicate activator on the rheology, geopolymerization and strength of fly ash/slag geopolymer pastes. Cem Concr Compos. https://doi.org/10.1016/j.cemconcomp.2018.12.007
25. Jeon D, Yum WS, Jeong Y, Oh JE (2018) Properties of quicklime(CaO)-activated Class F fly ash with the use of CaCl2. Cem Concr Res 111:147–156. https://doi.org/10.1016/j.cemconres.2018.05.019
26. Velandia DF, Lynsdale CJ, Provis JL, Ramirez F (2018) Effect of mix design inputs, curing and compressive strength on the durability of Na2SO4-activated high volume fly ash concretes. Cem Concr Compos 91:11–20. https://doi.org/10.1016/j.cemconcomp.2018.03.028
27. Zhou WJ, Lin S (2012) Influence of the MB value of manufactured sand on the mechanical property of concrete. New materials, applications and processes. Trans Tech Publications, Stafa-Zurich, pp 1352–1357
28. Shen W, Liu Y, Wang Z et al (2018) Influence of manufactured sand's characteristics on its concrete performance. Constr Build Mater 172:574–583. https://doi.org/10.1016/j.conbuildmat.2018.03.139
29. IS 2386 (2002). Method of test for aggregate for concrete. Indian Standard Institute, New Delhi, India
30. Sathanandam T, Awoyera PO, Vijayan V, Sathishkumar K (2017) Low carbon building: Experimental insight on the use of fly ash and glass fibre for making geopolymer concrete. Sustain Environ Res 27. https://doi.org/10.1016/j.serj.2017.03.005
31. Sateshkumar S, Awoyera P, Kandasamy T et al (2018) Impact resistance of high strength chopped basalt fibre-reinforced concrete. Rev la Construcción J Constr 17:240–249
32. ASTM C618 (2008). Standard Specification for Coal Fly Ash and Raw or Calcined Natural Pozzolan for Use in Concrete. Am Soc Test Material, Philadelphia, USA
33. EFNARC (2005). The European guidelines for self-compacting concrete. Surrey, GU9 7EN, UK
34. IS: 516–1959 Methods of test for strength of concrete. Indian Standard Institute, New Delhi, India

35. ASTM C469 / C469M (2014) Standard Test method for static modulus of elasticity and Poisson's ratio of concrete in compression. Am Soc Test Material, Philadelphia, USA
36. Siddique R (2011) Properties of self-compacting concrete containing class F fly ash. Mater Des 32:1501–1507. https://doi.org/10.1016/j.matdes.2010.08.043
37. Saha AK (2018) Effect of class F fly ash on the durability properties of concrete. Sustain Environ Res 28:25–31. https://doi.org/10.1016/j.serj.2017.09.001
38. Shen W, Yang Z, Cao L et al (2016) Characterization of manufactured sand: Particle shape, surface texture and behavior in concrete. Constr Build Mater 114:595–601. https://doi.org/10.1016/j.conbuildmat.2016.03.201